JBC Papers in Press. Published on September 20, 2012 as Manuscript M112.412320
The latest version is at http://www.jbc.org/cgi/doi/10.1074/jbc.M112.412320

Human and mouse Type I Natural Killer T-cell antigen receptors exhibit different fine specificities for CD1d-antigen

Kwok S. Wun[1], Fiona Ross[2], Onisha Patel[1], Gurdyal S. Besra[3], Steven A. Porcelli[4], Stewart K. Richardson[5], Santosh Keshipeddy[5], Amy R. Howell[5], Dale I. Godfrey[2#] & Jamie Rossjohn[1#]

[1] ARC Centre of Excellence in Structural and Functional Microbial Genomics, Department of Biochemistry and Molecular Biology, School of Biomedical Sciences, Monash University, Clayton, Victoria 3800, Australia.

[2]Department of Microbiology & Immunology, University of Melbourne, Parkville, Victoria 3010, Australia.

[3]School of Biosciences, University of Birmingham, Edgbaston, Birmingham B15 2TT, UK.

[4]Department of Microbiology and Immunology, Albert Einstein College of Medicine, Room 416 Forchheimer Building, 1300 Morris Park Avenue, Bronx, NY, USA, 10461.

[5]Department of Chemistry, University of Connecticut, Storrs, Connecticut 06269 3060, USA
[#]Joint senior &corresponding authors

*Running title: *Human NKT TCR recognition.*

[#]To whom correspondence should be addressed: Jamie Rossjohn, jamie.rossjohn@monash.edu Dept. of Biochemistry & Molecular Biology, School of Biomedical Sciences, Monash University, Clayton, Vic 3800, Australia, Tel: (613) 99029236 Fax: (613) 99025000; and Dale Godfrey, godfrey@unimelb.edu.au Dept. of Microbiology, University of Melbourne, Parkville, Vic 3010, Australia, Tel: (613) 8344 5689 Fax: (613) 93471540

Keywords: Natural Killer T cells; T cell antigen receptors; CD1d; glycolipid

Background: Natural Killer T cell antigen receptors (NKT TCRs) are restricted to lipid antigens presented by CD1d.
Results: Fine specificity differences between human and mouse NKT TCRs towards CD1d-antigen complexes were observed.
Conclusion: A structural basis underpins the fine specificity differences between human and mouse NKT TCRs.
Significance: Understanding human NKT cell response to CD1d-restricted antigens has important therapeutic implications in developing NKT cell agonists.

SUMMARY

Human and mouse type I NKT cells respond to a variety of CD1d-restricted glycolipid antigens (Ags), with their NKT cell antigen receptors (NKT TCRs) exhibiting reciprocal cross-species reactivity that is underpinned by a conserved NKT TCR-CD1d-Ag docking mode. Within this common docking footprint, the NKT TCR recognises, to varying degrees of affinity, a range of Ags. Presently it is unclear whether the human NKT TCRs will mirror the generalities underpinning the fine specificity of the mouse NKT TCR-CD1d-Ag interaction. Here, we assessed human NKT TCR recognition against altered glycolipid ligands of α-galactosylceramide (α-GalCer), and have determined the structures of a human NKT TCR in complex with CD1d-4′,4′′-deoxy-α-GalCer and CD1d-α-GalCer with a shorter, di-unsaturated acyl chain (C20:2). AGLs with acyl-chain modifications did not affect the affinity of the human NKT TCR-CD1d-Ag interaction. Surprisingly, human NKT TCR recognition is more tolerant to modifications at the 4′-OH position in comparison to the 3′-OH position of α-GalCer, which contrasts the fine specificity of the mouse NKT TCR-CD1d-Ag recognition (4′-OH > 3′-OH). The fine specificity differences between human and mouse NKT TCRs was attributable to differing interactions between the respective complementarity determining region (CDR) 1α loops and the Ag. Accordingly,

Copyright 2012 by The American Society for Biochemistry and Molecular Biology, Inc.

germline encoded fine-specificity differences underpin human and mouse type I NKT TCR interactions, which is an important considerations for therapeutic development and NKT cell physiology.

INTRODUCTION

NKT cells are CD1d restricted, lipid antigen-reactive T cells that are present in mice and humans. The most extensively studied NKT cells, known as type I NKT cells, are defined by their expression of an invariant TCRα chain (Vα24Jα18 in humans, and the orthologous Vα14Jα18 in mice) paired with a limited range of TCRβ chains (Vβ11 in humans, Vβ8, Vβ7 or Vβ2 in mice) (1). Type I NKT cells are also defined by their ability to recognize the synthetic glycolipid antigen α-galactosylceramide (α-GalCer) presented by CD1d(2). Type II NKT cells, by contrast, do not express the invariant TCRα chain that characterizes type I NKT cells, nor do they recognize α-GalCer, and can adopt distinct CD1d-Ag docking modes compared to type I NKT TCRs(3-5). This study will focus on type I NKT cells, which from here on will simply be referred to as NKT cells.

The structures of human and mouse NKT TCRs have been solved with a variety of CD1d-restricted Ags, including α-GalCer and analogues thereof, microbial ligands, phospholipid Ags and β-linked self-Ags(6-18). Collectively, these NKT TCR-CD1d-Ag complexes exhibited a conserved docking strategy in which the NKT TCR adopted a parallel docking mode above the F′-pocket of the CD1d Ag-binding cleft (19-24). Within this common footprint the NKT TCR α-chain dominated the interaction, binding to CD1d and Ag, whereas the β-chain exclusively contacted CD1d. Nevertheless, variations on a theme were apparent, in that there were differing roles of the Complementarity Determining Regions (CDR) loops of the NKT TCRs for some CD1d-Ag complexes (13,14,25). For example, NKT TCR-CD1d autoreactivity seems attributable to a greater role of the CDR3β loop, and altered juxtapositioning of the Vβ8/7/2 chains results in differing Vβ-mediated footprints that can impact on Vα-Jα interactions with the CD1d-Ag (6,16,21). Moreover, alterations in the Vα and/or Vβ usage within the NKT TCR can impact on the specificity towards CD1d-restricted Ags. For example, the Vα10 NKT TCR preferentially recognizes α-glucosylceramide (α-GlcCer) over α-GalCer (26), while Vβ7 NKT TCRs preferentially respond to iGb3 and α-GlcCer (9) (27,28). Moreover, Vα24+ and Vα24- NKT TCRs can respond differently to α-GalCer and the closely related α-GlcCer(29).

While NKT cells are activated by a range of CD1d-restricted Ags, they also discriminate between closely related Ags (termed altered glycolipid ligands, AGLs) to generate distinct functional responses. For example, while some antigens can promote T_H1 biased responses downstream of NKT cell activation, others generate T_H2 biased responses (30,31). Recently, we provided insight into mouse NKT TCR fine specificity against a panel α-GalCer AGLs (9). The Vβ8.2 NKT TCRs were more sensitive to alterations at the 4′-OH position in comparison to the 3′-OH position of the galactosyl headgroup, and $Vβ7^+$ NKT TCRs preferentially proliferated to AGLs with modifications in the 4′-OH position. Studies using AGLs highlight the feasibility of manipulating the NKT cell response for therapeutic gain (reviewed in (32)). However, to enable more rationally-designed NKT-based therapeutics requires an understanding of the structural basis of antigenic modulation of the human NKT cell response. While the Jα18-encoded loop is identical in the mouse and human NKT TCRs, sequence differences reside in the corresponding Vα14 and Vα24 chains, which is notable given that the CDR1α loop contacts the lipid Ag(6,18,33). Accordingly, we asked whether these differences in the Vα chains manifest in differing fine specificity profiles between the human and mouse NKT TCRs. We demonstrate that, in contrast to mouse NKT TCR reactivity, the human NKT TCRs are more tolerant towards modifications at the 4′-OH of α-GalCer, yet are very sensitive to modifications in the 3′-OH motif. Accordingly, our data demonstrate that notable fine specificity differences exist between human and mouse NKT cells, despite the high level of identity between these respective NKT TCRs.

EXPERIMENTAL PROCEDURES

Glycolipids

The glycolipid analogues used in this study have been previously described (9,23,31,34).

Flow cytometry based affinity studies

Human CD1d tetramers were loaded with specific glycolipids used to label NKT cells from samples of human PBMC. Human samples were derived from The Red Cross Blood Bank with ethics approvals from Red Cross and University of Melbourne Human Ethics Committee (Ethics Application ID 1035100.1). Samples were selected based on NKT cell percentages being higher than 0.03%. In some experiments, NKT cells were enriched by CD1d-α-GalCer tetramer-phycoerythrin (PE) staining followed by enrichment using MACS-anti-PE beads and running over a MACS column (Miltenyi Biotec). Enriched NKT cells were then sorted on a FACSaria (Becton Dickinson) and then stimulated for 2 days in the presence of plate bound anti-CD3 (clone UCHT1, 10μg/ml), soluble anti-CD28 (clone CD28.2, 10μg/ml), phytohemagglutinin (PHA, 0.5 μg/ml) plus recombinant human IL-2 (100 U/ml, Peprotech) and IL-7 (50 ng/ml, eBioscience). After 2 days, NKT cells were washed and expanded in the presence of IL-2 and IL-7 but in the absence of further anti-CD3/CD28 stimulation for 2-3 weeks. In other experiments, fresh NKT cells were directly examined without in vitro expansion. For analysis of cultured or fresh NKT cells, cells were labelled with 7-AAD viability dye (Sigma), anti-Vβ11 (Beckman Coulter, clone C21), CD3 (eBiosceince, clone UCHT1), and CD1d tetramer loaded with various glycolipids. Fresh NKT cells were electronically enriched by gating on Vβ11+ cells, then fresh and enriched NKT cells were examined for CD1d tetramer staining (mean fluorescence intensity, MFI) over a range of dilutions.

Purification of Vα24 NKT TCRs and CD1d-Ag

The method for cloning, expression, and purification of the human Vα24 NKT TCRs and human CD1d has been previously described (35). Lipid loading of CD1d was performed as described previously (6).

Protein crystallization, structure determination, and refinement

Purified human NKT TCR-CD1d-glycolipid complexes were concentrated to 10 mg/ml and crystals were obtained at room temperature after 7 days via the hanging drop vapour diffusion technique with equal protein:mother-liquor ratio. Crystals of the α-GalCer (C20:2) ternary complex were grown in 8% polyethylene glycol 10K, 0.2 M magnesium chloride, and 0.1 M Tris, pH 8.8, and flash frozen in the mother-liquor containing 25% polyethylene glycol 10K as cryoprotectant. Crystals of the 4′,4′′-deoxy-α-GalCer ternary complex were grown in 9% polyethylene glycol 10K, 0.2 M magnesium chloride, and 0.1 M glycine, pH 10.0, and flash frozen in the mother-liquor containing 30% polyethylene glycol 10K as cryoprotectant.

Data for the human NKT TCR-CD1d-α-GalCer (C20:2) and 4′,4′′-deoxy-α-GalCer ternary complexes were collected at the Advanced Photon Source facility, Chicago, and the Australian Synchrotron Facility in Melbourne, Australia, respectively. Data was processed with programs from the *CCP4 suite* (36). Crystals of the ternary complexes diffracted to a range of 2.9 Å - 3.1 Å, and belong to the space group C222. Crystal structures of the NKT TCR-CD1d-glycolipid complexes were solved via Phaser using the 2.5 Å human NKT TCR-CD1d-α-GalCer complex (Protein Data Bank ID code 3HUJ) minus α-GalCer as the search model(6). To prevent model bias, the simulated annealing protocol in Phenix (37) was applied in the initial structure refinement. Glycolipid libraries were generated via the program Sketcher within the CCP4 suite, and the glycolipid models were subsequently built into the work models. Restrained refinement followed by the inclusion of translation libration screw parameters at the combined with rounds of model building with Coot (38) were used to improve the work model as monitored by the R_{free} values. Programs within the CCP4 suite were utilized to assess the quality of the structures. For data collection and refinement statistics, see Table 1). All molecular graphics illustrations were generated using PyMol (39).
PDB Accession codes:
The coordinates for the NKT TCR-CD1d-Ag complexes have been deposition in the Protein Data Bank.

Surface plasmon resonance measurements and analysis

The surface plasmon resonance (SPR) experiments were conducted at 25°C on a

Biacore 3000 instrument using HBS buffer (10 mM HEPES-HCl (pH 7.4), 150 mM NaCl, and 0.005% surfactant P20) and have been previously described (23,35). Approximately 3000 RU of biotinylated CD1d-glycolipids were coupled to a SA sensor chip and analyzed against a two-fold serial dilution of the NKT TCRs. Concentration series for the α-GalCer, α-GalCer (C20:2), α-GlcCer (C20:2), 3′,4′′-deoxy and 4′,4′′-deoxy-α-GalCer glycolipids ranged from 39 nM to 40 μM, and for α-GlcCer glycolipid ranged from 98 nM to 25 μM. The analyte was passed over the sensor chip at 5 μl/min for 80s at 25°C, and the final response was subtracted from that of the unloaded CD1d. The affinity value was determined using the BIAevaluation software and sensorgram plots were presented using GraphPad Prism. All experiments were carried out in duplicate.

RESULTS

Human NKT cells show differential reactivity with distinct α-GalCer AGLs

We have previously observed that mouse NKT cells show differential recognition of α-GalCer AGLs with a high sensitivity to modifications in the 4′-OH moiety as detected using 4′,4′′-deoxy α-GalCer and α-GlcCer (9,16). To determine whether human NKT cells exhibit a similar fine specificity pattern, we used a CD1d tetramer dilution approach where CD1d tetramers were loaded with α-GalCer AGLs that varied in the composition of the galactosyl headgroup (3′,4′′-deoxy-α-GalCer, 4′,4′′-deoxy-α-GalCer, α-GlcCer (C20:2) and the acyl chain, α-GalCer (C20:2) (Figure 1). The 3′,4′′-deoxy-α-GalCer and 4′,4′′-deoxy-α-GalCer analogues lack their 3′-OH and 4′-OH on the sugar moiety respectively, and both also lack the OH group at position 4 of the sphingoid base. The latter modification has been shown not to impact on NKT TCR recognition(9,16), and thus the impact of the 3′,4′′-deoxy-α-GalCer and 4′,4′′-deoxy-α-GalCer AGLs can be attributed to the modifications in the galactosyl headgroup. These tetramers were used to measure staining intensity of heterogeneous human NKT cells. Two approaches were used – firstly, human NKT cells were enriched and expanded *in vitro* for 2-3 weeks prior to tetramer staining. The results demonstrated some unexpected differences between the fine specificity of mouse and human NKT cells. While the mean fluorescence intensities were highest for α-GalCer, and α-GalCer (C20:2), modifications to the 4′-OH sugar moiety associated with 4′,4′′-deoxy-α-GalCer and α-GlcCer (C20:2), resulted in only a slight reduction in staining intensity. In contrast, 3′,4′′-deoxy α-GalCer labelling intensity was much lower and similar to unloaded (endogenous Ag loaded) CD1d tetramer, which suggested that the 3′-OH moiety is critical for human NKT TCR recognition of α-GalCer (Figure 2A and B). To ensure that the MACS enrichment and *in vitro* expansion had not biased the TCR usage of the NKT cells, fresh NKT cells from 3 separate blood donors (Figure 2C and D) were tested. A similar pattern was observed with freshly isolated NKT cells, where tetramer staining was almost completely abrogated with the 3′,4′′-deoxy-α-GalCer AGL, while tetramer loaded with 4′,4′′-deoxy-α-GalCer and α-GlcCer (C20:2) caused only a slightly reduced intensity. Thus, these results suggest that human NKT cells are far more sensitive to modifications to the 3′-OH moiety, and relatively tolerant of modifications to the 4′-OH moiety, in contrast to mouse NKT cells.

Affinity measurements

While the Vα14Vβ8.2 NKT TCR binds to CD1d-α-GalCer with high affinity (K_{Deq} ≈ 60nM) (6,9), we previously established that the corresponding Vα24Vβ11 NKT TCR-CD1d-α-GalCer interaction was notably weaker (K_{Deq} ≈ 460 nM) (23). Moreover, previous measurements using a distinct Vα24Vβ11 NKT TCR indicated that the interaction with CD1d-α-GalCer was even weaker (K_{Deq} ≈ 7 μM) (40). The reasons for the differences in the affinity values of the two distinct NKT TCRs is unclear, but maybe attributable to different methodologies in CD1d-α-GalCer purification or differing CDR3β usage (40) (23). Regardless, the observations suggest differing recognition characteristics of the mouse and human NKT TCRs. To address this we firstly confirmed the relatively lower affinity of the Vα24Vβ11 (NKT15) NKT TCR-CD1d-α-GalCer interaction (K_{Deq} ≈ 430 nM), and that cross-species reactivity onto mouse CD1d-α-GalCer was further reduced (K_{Deq} ≈ 1.5 μM).

Previously we had characterised two other human NKT TCRs that differed only in their CDR3β composition (NKT12, and NKT18), and established that the CDR3β variability exhibited by these three human NKT TCRs either did not impact (NKT12), or impacted moderately (NKT18) on the CD1d-α-GalCer interaction (K_{Deq} for NKT12 and NKT18 was approximately 430nM and 940nM respectively) (35).

Next to address the fine specificity of the human NKT TCRs (NKT12, NKT15 and NKT18), we determined their affinity towards the panel of AGLs (Figure 1, Figure 3, Table 2). Consistent with the mouse NKT TCR affinity measurements, and with the human CD1d-tetramer staining (Figure 2), the AGL with the acyl chain modification, α-GalCer (C20:2), moderately affected the affinity of the interaction ($K_{Deq} \approx 740$ nM). Thus, analogous to mouse NKT cell reactivity, we suggest that acyl chain modifications that impact on human NKT cell activity is more likely attributable to mechanisms centered on Ag-loading/presentation(41). The affinity measurements confirmed that modifications at the 4′-OH position of α-GalCer (4′,4′′-deoxy and α-GlcCer (C20:2)) have moderate impact on the human NKT TCR affinity (K_{Deq} of 830 nM and 320 nM respectively), indicating that the 4′-OH moiety is dispensable for the human NKT TCR-CD1d-α-GalCer interaction. Consistent with the CD1d-tetramer staining data (Figure 2), the affinity of human NKT TCR for 3′,4′′-deoxy-α-GalCer was markedly lower ($K_{Deq} \approx 10\mu m$), confirming that the 3′-OH position was a critical determinant for human NKT TCR reactivity. Further, the heightened dependency of the 3′-OH position was also observed for the NKT12 and the NKT18 TCRs, whereas modifications in the 4′-OH group had a lesser impact (Table 2).

Accordingly, in contrast to mouse NKT TCR recognition of CD1d-α-GalCer, the 3′-OH position of α-GalCer is a critical determinant for human NKT TCR recognition.

The NKT TCR-CD1d-α-GalCer (C20:2) and 4′,4′′-deoxy complexes

To provide a structural basis of the human NKT TCR fine specificity, we determined the structure of the NKT15 TCR in complex with CD1d-α-GalCer (C20:2) and CD1d-4′,4′′-deoxy-α-GalCer (Table 1). These NKT TCR-CD1d-Ag complexes crystallized in the same space group with similar unit cell dimensions, and were refined to a comparable resolution limit and refinement statistics and unless explicitly stated, the electron density at the NKT TCR-CD1d interface was readily interpretable (Supplementary Figure 1). In both complexes, the NKT TCR adopted the canonical docking mode observed for the human NKT TCR-CD1d-α-GalCer complex (6,7), indicating that the AGLs did not cause a re-positioning of the human NKT TCR (Figure 4). Thus, the NKT TCR bound approximately parallel to, and above, the F′-pocket of the CD1d-Ag binding cleft.

For the two AGL ternary complexes, the buried surface area (BSA) upon complexation was ≈ 850-870 Å^2, which compares closely to the BSA value of ≈ 890 Å^2 at the human NKT TCR-CD1d-α-GalCer interface (7) (6). This indicates that, relative to α-GalCer, no substantial alteration in the BSA upon ligation was observed in accommodating these two AGLs. For these complexes, as observed for the human NKT TCR-CD1d-α-GalCer interaction, the TCRα-chain contributed approximately three times more BSA than the TCRβ-chain, whereby the Vα24 and Jα18-encoded contacts were mediated by the CDR1α and CDR3α loops respectively (6). Further, the Vβ11 interactions were mediated primarily by the CDR2β loop interacting with the α1-helix of CD1d (approximately 20% BSA). This conserved network of CDR2β-mediated contacts included Tyr48β and Tyr50β interacting with Glu83 and Lys86 of CD1d, with the latter residue also forming van der Waals (vdw) contacts with Glu56β (Supplementary Table 1) (7). The CDR3β loop was located at the periphery at the interface, with one residue (Tyr103β), making vdw interactions with Gln150 from CD1d. The lack of substantial involvement of the CDR3β loop in contacting CD1d was consistent with the lack of impact of CDR3β variation in the staining of the total Vβ11 NKT cell population (Figure 2) and the similar binding affinity of the

NKT12 and NKT18 TCRs (Table 2).

α-GalCer (C20:2) differs from α-GalCer in its acyl chain, which resides within the A′-pocket of CD1d. In CD1d-α-GalCer, the tip of the 26C acyl tail curled back onto itself and formed intra-chain vdw interactions (42). Analogous to the crystal structure of the mouse NKT TCR-CD1d-α-GalCer (C20:2) complex (9), the electron density corresponding to the majority of the 20 acyl tail carbons were not well resolved in the human NKT TCR-CD1d-α-GalCer (C20:2) ternary complex, suggesting that the acyl chain is mobile within the A′-pocket through lack of the intra-stabilising interactions as observed for α-GalCer. Further, dissimilar to previous studies (43), no spacer lipid occupied the A′-pocket, presumably attributable to space restrictions. Nevertheless, the A′-pocket of CD1d, when bound to the α-GalCer (C20:2) adopted an essentially identical conformation when compared to NKT TCR-CD1d-α-GalCer. As such, the affinity of the NKT TCR-CD1d-α-GalCer (C20:2) interaction was matched closely to that of the NKT TCR-CD1d-α-GalCer interaction, and the interactions between that NKT TCR and the galactosyl headgroup at the respective interfaces were very similar. Namely, the galactosyl headgroup sat beneath the CDR1α loop and abutted the CDR3α loop. While the 6′-OH moiety was solvent exposed, the 2′-OH, 3′-OH and 4′-OH moieties were sequestered by the NKT TCR, with Gly96α and Phe29α making hydrogen bonds to the 2′-OH and 4′-OH of the galactose moiety respectively (Figure 5). Thus, the altered NKT proliferation response to α-GalCer (C20:2) is more attributable to factors such as altered lipid loading/presentation (41) (9).

The 4′,4′′-deoxy-α-GalCer AGL lacks the 4′-OH group on the galactosyl headgroup, and as a result the hydrogen bond with the CDR1α loop is absent. Despite this, there is minimal perturbation to the positioning of the galactosyl headgroup, in that it superposes very well onto α-GalCer. Possibly, the presence of Trp 153 in human CD1d (Gly 155 in mouse CD1d), which packs against the galactosyl ring, helps stabilise its conformation within the Ag-binding cleft, thereby reducing the impact of the 4′-OH modification. The lack of a significant structural impact of the 4′,4′′-deoxy-α-GalCer AGL was consistent with the minimal effect on the affinity of the interaction, and contrasts the effect observed in the mouse NKT TCR-CD1d-4′,4′′-deoxy-α-GalCer interaction(6). Here, the 4′-deoxy substitution caused a shift in the conformation of the galactosyl headgroup that resulted in a loss of interaction with Asn30α, a weakening of the hydrogen bond between the 3′-OH and Asn30α. Accordingly, the 4′-OH position has a major impact on mouse NKT TCR recognition(6,16) and conversely a modest impact on human NKT TCR recognition.

DISCUSSION

A high level of sequence and structural identity exists between the Vα24Jα18 NKT TCR and the orthologous mouse Vα14Jα18 NKT TCR (44), and consequently the structures of the corresponding NKT TCR-CD1d-α-GalCer complexes are very similar(6,7). This conservation is underpinned by the Jα18-encoded CDR3α loop, which contacts CD1d and the Ag, and the CDR2β loop from the Vβ chain, which in the Vβ11 and Vβ8.2 NKT TCRs, contains two tyrosine residues that sits above the F′-pocket of CD1d (6,7,19). Despite this consensus NKT TCR-CD1d docking, variations in the Vβ and CDR3β usage can modulate NKT TCR affinity and antigen specificity (6) (9,13,16).

A greater role in the Vα-encoded region in contacting the lipid Ag is evident in some NKT TCR-CD1d-Ag complexes (13,14), suggesting that sequence differences within the germline-encoded Vα regions of NKT TCRs can potentially impact on antigen specificity. For example, the mouse Vα10 NKT TCRs preferentially recognises α-GlcCer-containing ligands, whereupon the CDR1α and CDR2α loops play a role in contacting the Ag (26). Further, sequence differences in the CDR1α loop of the Vα14 and Vα24 NKT TCRs, suggested that mouse and human NKT TCRs may exhibit altered fine specificity profiles. Within the mouse NKT TCR-CD1d-α-GalCer complexes, the 3′-OH and 4′-OH moieties are sequestered by Asn30α, with the 4′-OH moiety of α-GalCer being more critical for the interaction than the 3′-OH moiety (9). This was

attributable to the modification of the 4′-OH position leading to a greater disruption in the number of contacts between the galactosyl headgroup and the NKT TCR in comparison to the 3′-OH modification.

The human NKT TCR was more tolerant to modifications at the 4′-OH position and less tolerant to modifications in the 3′-OH position of α-GalCer. Within the human NKT TCR-CD1d-α-GalCer complex, the 4′-OH group hydrogen bonds to the main chain of Phe29α, while the 3′-OH hydrogen bonds to Ser30α. The human NKT TCR-CD1d-4′,4′′-deoxy-α-GalCer complex showed that there were limited perturbations arising from the loss of the interaction between the 4′-OH moiety and Phe 29. While were not able to crystallize the NKT TCR-CD1d-3′,4′-deoxy-α-GalCer complex, we speculate that the 3′-OH modification results in a loss of the hydrogen bond with Ser30α. Further, the 3′-OH modification may result in a loss of interactions with the CDR3α loop and with Asp151 of hCD1d, which may impact on the Asp151-mediated interactions with the CDR3α loop. The tetramer staining and affinity measurements show that the human NKT TCR is much less tolerant to modifications in the 3′-OH moiety than the 4′-OH moiety. Surprisingly, the three human NKT TCRs examined exhibited modest differences in the responses to some of the AGLs, indicating that CDR3β differences can subtly indirectly impact on CD1d-Ag-recognition, analogous to that observed in the mouse NKT TCR system (22) (24).

Our findings show that the human Vα24NKT TCRs exhibit altered specificity profiles in comparison to the Vα14 NKT TCRs, and suggest that non-Vα24 NKT TCRs may exhibit altered fine specificity profiles (40). Our data also provides a basis for understanding the conserved use of the Jα18-encoded CDR3α loop in the non-Vα24 TCRs (29), and suggest that these TCRs will adopt a similar docking mode to that of the Vα24 NKT TCRs. Our results also suggest that glucose-containing glycolipids may be more antigenic towards human NKT cells. In line with this view, it was recently established that β-GlcCer was a ubiquitous self-Ag for mouse and human NKT cells, with this Ag being more reactive towards human NKT cells (45). Of additional interest, some bacterial glycolipids seem to use glucose-based headgroups suggesting that human NKT cells may be better at responding to such antigens (46,47). While the fundamental principles underscoring NKT TCR-CD1d-Ag recognition is conserved across mice and humans, fine specificity differences between the mouse and human NKT TCRs are apparent. Such differences are important for NKT cell physiology, and will be critically important to understand in the context of rationally developing human-based NKT cell therapeutics (48) (49).

REFERENCES

1. Godfrey, D. I., MacDonald, H. R., Kronenberg, M., Smyth, M. J., and Van Kaer, L. (2004) *Nat Rev Immunol* **4**, 231-237
2. Kawano, T., Cui, J., Koezuka, Y., Toura, I., Kaneko, Y., Motoki, K., Ueno, H., Nakagawa, R., Sato, H., Kondo, E., Koseki, H., and Taniguchi, M. (1997) *Science* **278**, 1626-1629
3. Rhost, S., Sedimbi, S., Kadri, N., and Cardell, S. L. (2012) *Scandinavian Journal of Immunology* **76**, 246-255
4. Girardi, E., Maricic, I., Wang, J., Mac, T.-T., Iyer, P., Kumar, V., and Zajonc, D. M. (2012) *Nat Immunol* **13**, 851-856
5. Patel, O., Pellicci, D. G., Gras, S., Sandoval-Romero, M. L., Uldrich, A. P., Mallevaey, T., Clarke, A. J., Le Nours, J., Theodossis, A., Cardell, S. L., Gapin, L., Godfrey, D. I., and Rossjohn, J. (2012) *Nat Immunol* **13**, 857-863
6. Pellicci, D. G., Patel, O., Kjer-Nielsen, L., Pang, S. S., Sullivan, L. C., Kyparissoudis, K., Brooks, A. G., Reid, H. H., Gras, S., Lucet, I. S., Koh, R., Smyth, M. J., Mallevaey, T., Matsuda, J. L., Gapin, L., McCluskey, J., Godfrey, D. I., and Rossjohn, J. (2009) *Immunity* **31**, 47-59
7. Borg, N. A., Wun, K. S., Kjer-Nielsen, L., Wilce, M. C., Pellicci, D. G., Koh, R., Besra, G. S., Bharadwaj, M., Godfrey, D. I., McCluskey, J., and Rossjohn, J. (2007) *Nature* **448**, 44-49

8. Yu, E. D., Girardi, E., Wang, J., and Zajonc, D. M. (2011) *The Journal of Immunology* **187**, 2079-2083
9. Wun, K. S., Cameron, G., Patel, O., Pang, S. S., Pellicci, D. G., Sullivan, L. C., Keshipeddy, S., Young, M. H., Uldrich, A. P., Thakur, M. S., Richardson, S. K., Howell, A. R., Illarionov, P. A., Brooks, A. G., Besra, G. S., McCluskey, J., Gapin, L., Porcelli, S. A., Godfrey, D. I., and Rossjohn, J. (2011) *Immunity* **34**, 327-339
10. Aspeslagh, S., Li, Y., Yu, E. D., Pauwels, N., Trappeniers, M., Girardi, E., Decruy, T., Van Beneden, K., Venken, K., Drennan, M., Leybaert, L., Wang, J., Franck, R. W., Van Calenbergh, S., Zajonc, D. M., and Elewaut, D. (2011) *Embo J* **30**, 2294-2305
11. Li, Y., Girardi, E., Wang, J., Yu, E. D., Painter, G. F., Kronenberg, M., and Zajonc, D. M. (2010) *The Journal of Experimental Medicine* **207**, 2383-2393
12. Kerzerho, J., Yu, E. D., Barra, C. M., Alari-Pahisa, E., Girardi, E., Harrak, Y., Lauzurica, P., Llebaria, A., Zajonc, D. M., Akbari, O., and Casta√±o, A. R. l. (2012) *The Journal of Immunology* **188**, 2254-2265
13. Mallevaey, T., Clarke, A. J., Scott-Browne, J. P., Young, M. H., Roisman, L. C., Pellicci, D. G., Patel, O., Vivian, J. P., Matsuda, J. L., McCluskey, J., Godfrey, D. I., Marrack, P., Rossjohn, J., and Gapin, L. (2011) *Immunity* **34**, 315-326
14. Pellicci, D. G., Clarke, A. J., Patel, O., Mallevaey, T., Beddoe, T., Le Nours, J., Uldrich, A. P., McCluskey, J., Besra, G. S., Porcelli, S. A., Gapin, L., Godfrey, D. I., and Rossjohn, J. (2011) *Nat Immunol* **12**, 827-833
15. Girardi, E., Yu, E. D., Li, Y., Tarumoto, N., Pei, B., Wang, J., Illarionov, P., Kinjo, Y., Kronenberg, M., and Zajonc, D. M. (2011) *PLoS biology* **9**, e1001189
16. Patel, O., Pellicci, D. G., Uldrich, A. P., Sullivan, L. C., Bhati, M., McKnight, M., Richardson, S. K., Howell, A. R., Mallevaey, T., Zhang, J., Bedel, R., Besra, G. S., Brooks, A. G., Kjer-Nielsen, L., McCluskey, J., Porcelli, S. A., Gapin, L., Rossjohn, J., and Godfrey, D. I. (2011) *Proceedings of the National Academy of Sciences* **108**, 19007-19012
17. Patel, O., Cameron, G., Pellicci, D. G., Liu, Z., Byun, H. S., Beddoe, T., McCluskey, J., Franck, R. W., Castano, A. R., Harrak, Y., Llebaria, A., Bittman, R., Porcelli, S. A., Godfrey, D. I., and Rossjohn, J. (2011) *Journal of Immunology* **187**, 4705-4713
18. Lopez-Sagaseta, J., Sibener, L. V., Kung, J. E., Gumperz, J., and Adams, E. J. (2012) *The EMBO journal* **31**, 2047-2059
19. Godfrey, D. I., Rossjohn, J., and McCluskey, J. (2008) *Immunity* **28**, 304-314
20. Scott-Browne, J. P., Matsuda, J. L., Mallevaey, T., White, J., Borg, N. A., McCluskey, J., Rossjohn, J., Kappler, J., Marrack, P., and Gapin, L. (2007) *Nat Immunol* **8**, 1105-1113
21. Godfrey, D. I., Pellicci, D. G., Patel, O., Kjer-Nielsen, L., McCluskey, J., and Rossjohn, J. (2010) *Semin Immunol* **22**, 61-67
22. Florence, W. C., Xia, C., Gordy, L. E., Chen, W., Zhang, Y., Scott-Browne, J., Kinjo, Y., Yu, K. O., Keshipeddy, S., Pellicci, D. G., Patel, O., Kjer-Nielsen, L., McCluskey, J., Godfrey, D. I., Rossjohn, J., Richardson, S. K., Porcelli, S. A., Howell, A. R., Hayakawa, K., Gapin, L., Zajonc, D. M., Wang, P. G., and Joyce, S. (2009) *EMBO J* **28**, 3579-3590
23. Wun, K. S., Borg, N. A., Kjer-Nielsen, L., Beddoe, T., Koh, R., Richardson, S. K., Thakur, M., Howell, A. R., Scott-Browne, J. P., Gapin, L., Godfrey, D. I., McCluskey, J., and Rossjohn, J. (2008) *The Journal of Experimental Medicine* **205**, 939-949
24. Mallevaey, T., Scott-Browne, J. P., Matsuda, J. L., Young, M. H., Pellicci, D. G., Patel, O., Thakur, M., Kjer-Nielsen, L., Richardson, S. K., Cerundolo, V., Howell, A. R., McCluskey, J., Godfrey, D. I., Rossjohn, J., Marrack, P., and Gapin, L. (2009) *Immunity* **31**, 60-71
25. Matulis, G., Sanderson, J. P., Lissin, N. M., Asparuhova, M. B., Bommineni, G. R., Schumperli, D., Schmidt, R. R., Villiger, P. M., Jakobsen, B. K., and Gadola, S. D. (2010) *PLoS Biol* **8**, e1000402
26. Uldrich, A. P., Patel, O., Cameron, G., Pellicci, D. G., Day, E. B., Sullivan, L. C., Kyparissoudis, K., Kjer-Nielsen, L., Vivian, J. P., Cao, B., Brooks, A. G., Williams, S. J., Illarionov, P., Besra, G. S., Turner, S. J., Porcelli, S. A., McCluskey, J., Smyth, M. J., Rossjohn, J., and Godfrey, D. I. (2011) *Nat Immunol* **12**, 616-623
27. Schumann, J., Mycko, M. P., Dellabona, P., Casorati, G., and Macdonald, H. R. (2006) *J Immunol* **176**, 2064-2068

28. Wei, D. G., Curran, S. A., Savage, P. B., Teyton, L., and Bendelac, A. (2006) *The Journal of Experimental Medicine* **203**, 1197-1207
29. Brigl, M., van den Elzen, P., Chen, X., Meyers, J. H., Wu, D., Wong, C.-H., Reddington, F., Illarianov, P. A., Besra, G. S., Brenner, M. B., and Gumperz, J. E. (2006) *The Journal of Immunology* **176**, 3625-3634
30. Miyamoto, K., Miyake, S., and Yamamura, T. (2001) *Nature* **413**, 531-534
31. Yu, K. O., Im, J. S., Molano, A., Dutronc, Y., Illarionov, P. A., Forestier, C., Fujiwara, N., Arias, I., Miyake, S., Yamamura, T., Chang, Y. T., Besra, G. S., and Porcelli, S. A. (2005) *Proc Natl Acad Sci U S A* **102**, 3383-3388
32. Cerundolo, V., Silk, J. D., Masri, S. H., and Salio, M. (2009) *Nat Rev Immunol* **9**, 28-38
33. Borg, N. A., Kjer-Nielsen, L., McCluskey, J., and Rossjohn, J. (2007) *Adv Exp Med Biol* **598**, 20-34
34. Raju, R., Castillo, B. F., Richardson, S. K., Thakur, M., Severins, R., Kronenberg, M., and Howell, A. R. (2009) *Bioorganic & Medicinal Chemistry Letters* **19**, 4122-4125
35. Kjer-Nielsen, L., Borg, N. A., Pellicci, D. G., Beddoe, T., Kostenko, L., Clements, C. S., Williamson, N. A., Smyth, M. J., Besra, G. S., Reid, H. H., Bharadwaj, M., Godfrey, D. I., Rossjohn, J., and McCluskey, J. (2006) *J Exp Med* **203**, 661-673
36. CCP4. (1994) *Acta Crystallogr D Biol Crystallogr* **50**, 760-763
37. Zwart, P. H., Afonine, P. V., Grosse-Kunstleve, R. W., Hung, L. W., Ioerger, T. R., McCoy, A. J., McKee, E., Moriarty, N. W., Read, R. J., Sacchettini, J. C., Sauter, N. K., Storoni, L. C., Terwilliger, T. C., and Adams, P. D. (2008) *Methods Mol Biol* **426**, 419-435
38. Emsley, P., and Cowtan, K. (2004) *Acta Crystallogr D Biol Crystallogr* **60**, 2126-2132
39. DeLano, W. L. (2002) *http://www.pymol.org*
40. Gadola, S. D., Koch, M., Marles-Wright, J., Lissin, N. M., Shepherd, D., Matulis, G., Harlos, K., Villiger, P. M., Stuart, D. I., Jakobsen, B. K., Cerundolo, V., and Jones, E. Y. (2006) *J Exp Med* **203**, 699-710
41. Im, J. S., Arora, P., Bricard, G., Molano, A., Venkataswamy, M. M., Baine, I., Jerud, E. S., Goldberg, M. F., Baena, A., Yu, K. O., Ndonye, R. M., Howell, A. R., Yuan, W., Cresswell, P., Chang, Y. T., Illarionov, P. A., Besra, G. S., and Porcelli, S. A. (2009) *Immunity* **30**, 888-898
42. Koch, M., Stronge, V. S., Shepherd, D., Gadola, S. D., Mathew, B., Ritter, G., Fersht, A. R., Besra, G. S., Schmidt, R. R., Jones, E. Y., and Cerundolo, V. (2005) *Nat Immunol* **6**, 819-826
43. Schiefner, A., Fujio, M., Wu, D., Wong, C.-H., and Wilson, I. A. (2009) *Journal of Molecular Biology* **394**, 71-82
44. Lantz, O., and Bendelac, A. (1994) *J Exp Med* **180**, 1097-1106
45. Brennan, P. J., Tatituri, R. V., Brigl, M., Kim, E. Y., Tuli, A., Sanderson, J. P., Gadola, S. D., Hsu, F. F., Besra, G. S., and Brenner, M. B. (2011) *Nature Immunology* **12**, 1202-1211
46. Kinjo, Y., Illarionov, P., Vela, J. L., Pei, B., Girardi, E., Li, X., Li, Y., Imamura, M., Kaneko, Y., Okawara, A., Miyazaki, Y., Gomez-Velasco, A., Rogers, P., Dahesh, S., Uchiyama, S., Khurana, A., Kawahara, K., Yesilkaya, H., Andrew, P. W., Wong, C. H., Kawakami, K., Nizet, V., Besra, G. S., Tsuji, M., Zajonc, D. M., and Kronenberg, M. (2011) *Nat Immunol* **12**, 966-974
47. Kinjo, Y., and Kronenberg, M. (2005) *J Clin Immunol* **25**, 522-533
48. Cerundolo, V., Barral, P., and Batista, F. D. (2010) *Current Opinion in Immunology* **22**, 417-424
49. Venkataswamy, M. M., and Porcelli, S. A. (2010) *Semin Immunol* **22**, 68-78

Acknowledgements-We wish to thank the synchrotron staff at the Advanced Photon Source and the Australian synchrotron for assistance with data collection and James McCluskey, Siew Siew Pang, Daniel Pellicci, Adam Uldrich and Meena Thakur for useful discussions and assistance. This research was supported by the National Health and Medical Research Council of Australia (NHMRC), the Australian Research Council (ARC) and the Cancer Council of Victoria. OP is supported by an ARC Future Fellowship, DIG is supported by an NHMRC Senior Principal Research Fellowship; JR is supported by an NHMRC Australia Fellowship**.**

FOOTNOTES

The abbreviations used are: α-GlcCer, α-galactosylceramide; Ags, antigens; CDR, complementarity determining region; SPR, surface plasmon resonance; TCRs, T cell antigen receptors

FIGURE LEGENDS

FIGURE 1. Schematics of α-GalCer and AGLs used in this study.

(A) α-GalCer, (B) α-GalCer (C20:2), (C) α-GlcCer (C20:2), (D) 3′,4′′-deoxy-α-GalCer, and (E) 4′,4′′-deoxy-α-GalCer.

FIGURE 2. CD1d tetramer staining of human NKT cells.

Peripheral blood mononuclear cells of two donors were expanded in vitro for 3 weeks and stained with: anti-CD3, anti-Vβ11 and serial dilutions of human CD1d tetramers loaded with α-GalCer, α-GalCer (C20:2), α-GlcCer (C20:2), 4′,4′′α-GalCer, 3′,4′′α-GalCer, or vehicle buffer (A and B). Representative flow cytometry plots are depicted for a 1:900 tetramer dilution for Donor 1 in (A) and the mean fluorescence intensity (MFI) data from all dilutions and all donors is plotted in (B). MFI depicts NKT cells derived from two patients studied in one experiment. Peripheral blood mononuclear cells were isolated from three donors (Donor 3, 4 and 5) and directly stained with: anti-CD3, anti-Vβ11 and serial dilutions of human CD1d tetramers loaded with α-GalCer, α-GalCer (C20:2), α-GlcCer (C20:2), 4′,4′′-α-GalCer, 3′,4′′-α-GalCer, or vehicle buffer. Vβ11+ CD3+ lymphocytes were electronically gated and the MFI of tetramer staining on the positive (upper region) was determined as shown at the 1:900 dilution for Donor 4 (C). MFI data from all 3 donors and all tetramer dilutions is plotted in (D). Data in D represents three different donors acquired over two experiments.

FIGURE 3. Binding analysis of the human NKT TCR and CD1d-AGLs interaction using surface plasmon resonance.

SPR sensograms demonstrating the interactions between the NKT15 TCR and human CD1d loaded with (A) α-GalCer, (B) α-GalCer (C20:2) (C) α-GlcCer (C20:2), (D) 3′,4′′-deoxy-α-GalCer, (E) 4′,4′′-deoxy-α-GalCer, and (F) mouse CD1d loaded with α-GalCer. Data represents duplicate runs from one experiment. (insets) the equilibrium response versus concentration series.

FIGURE 4. Structure overview of the human NKT TCRs-CD1d-AGLs complexes and their corresponding footprints.

(A) NKT15 TCR-CD1d-α-GalCer (PDB code 3HUJ). (B) NKT15 TCR-CD1d-4′,4′′-deoxy-α-GalCer. (C) NKT15 TCR-CD1d-α-GalCer (C20:2). Footprints are color-coded based on their CDR loop contributions. TCRα, purple; TCRβ, dark blue; CDR1α loop, yellow; CDR2α, beige, CDR3α loop, cyan; CDR1β, brown; CDR2β loop, orange; CDR3β loop, light green; CD1d heavy chain, green; β_2m, dark green; α-GalCer, magenta; C20:2, pink; 4′,4′-deoxy-α-GalCer, blue.

FIGURE 5. Comparison of the glycosyl headgroup interactions between the AGLs with the NKT15 TCR.

(A) α-GalCer, (B) 4′,4′′-deoxy-α-GalCer, (C) α-GalCer (C20:2). CDR1α loop, yellow; CDR3α loop, cyan; CD1d α-helices, green; α-GalCer, magenta; C20:2, pink; 4′,4′′-deoxy-α-GalCer, blue.(D) Superpositioning of the α-GalCer ternary complex (magenta) onto the 4′,4′′-deoxy-α-GalCer complex (blue) shows minimal repositioning of the glycosyl head group between the complexes.

Table 1. Data collection and refinement statistics

	NKT TCR-CD1d-α-GalCer (C20:2)	**NKT TCR-CD1d-4′,4′′-deoxy-α-GalCer**
Data Collection		
Temperature	100K	100K
Resolution limits (Å)	100-3.10 (3.27-3.10)	80-2.90 (3.06-2.90)
Space Group	C222	C222
Cell dimensions	*a*=145.93, *b*=176.91, *c*=82.95; α=β=γ=90°	*a*=144.27, *b*=177.26, *c*=83.75 ; α=β=γ=90°
Total N$^{o.}$ observations	239067	170626
N$^{o.}$ unique observations	19938	22894
Multiplicity	12.0 (12.2)	7.5 (7.7)
Data Completeness	100 (100)	99.9 (100)
I/σ	4.8 (2.1)	11.3 (2.4)
[1]R_{pim} (%)	11.6 (38.3)	9.4 (30.5)
Mosaicity	0.40	0.70
Refinement statistics		
[2]R_{factor} (%)	22.8	19.1
[3]R_{free} (%)	29.2	25.0
Non hydrogen atoms		
- protein	5869	6001
- lipid(s)	54	58
- water	17	20
- other	29	29
Ramachandran plot		
- Most favoured (%)	83.0	87.1
- Allowed region (%)	16.7	12.6
- Generously allowed region (%)	0.3	0.3
B-factors (Å^2)		
- Average main chain	70.9	72.5
- Average side chain	68.2	71.7
- lipid(s)	51.2	54.9
- water	35.2	57.2
rmsd bonds (Å)	0.003	0.005
rmsd angles (°)	0.714	0.903

[1]$R_{p.i.m} = \Sigma_{hkl} [1/(N-1)]^{1/2} \Sigma_i \left| I_{hkl,\, i} - \langle I_{hkl} \rangle \right| / \Sigma_{hkl} \langle I_{hkl} \rangle$

[2]$R_{factor} = \Sigma_{hkl} \left| \left| F_o \right| - \left| F_c \right| \right| / \Sigma_{hkl} \left| F_o \right|$ for all data except ≈ 5% which were used for [3]R_{free} calculation

Values in parentheses refer to the highest resolution bin

Table 2. Human NKT TCR affinity towards CD1d-Ag.

Ligand	NKT12 TCR	NKT15 TCR	NKT18 TCR
	K_{Deq} (μM)	K_{Deq} (μM)	K_{Deq} (μM)
hCD1d-α-GalCer	0.43 ± 0.03	0.43 ± 0.02	0.94 ± 0.04
hCD1d-α-GalCer (C20:2)	0.77 ± 0.09	0.74 ± 0.07	1.63 ± 0.12
hCD1d-α-GlcCer (C20:2)	0.34 ± 0.05	0.32 ± 0.05	0.76 ± 0.05
hCD1d-3′,4′′deoxy-α-GalCer	15.79 ± 0.52	8.96 ± 0.28	16.23 ± 0.46
hCD1d-4′,4′′deoxy-α-GalCer	0.93 ± 0.05	0.83 ± 0.03	1.90 ± 0.06
mCD1d-α-GalCer	2.83 ± 0.12	1.52 ± 0.08	2.31 ± 0.12

A

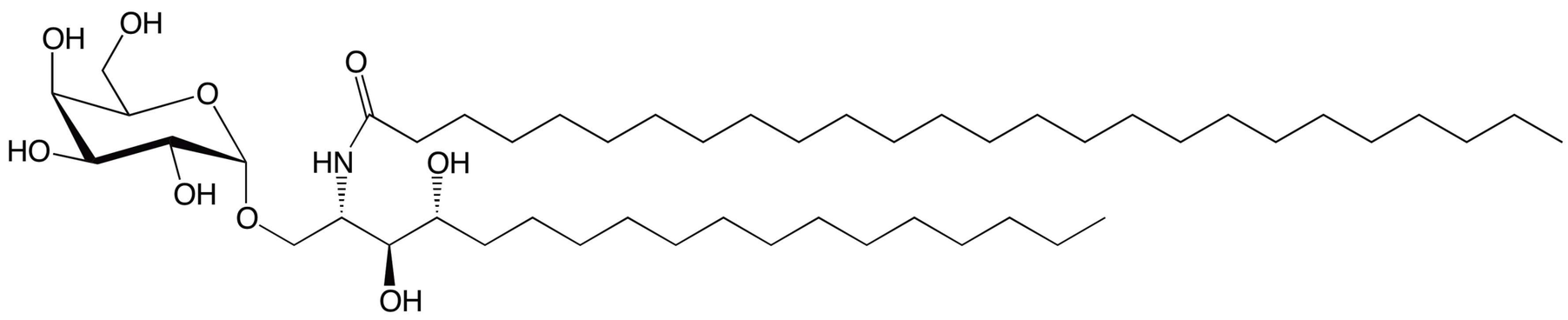

Acyl (C26)

Sphingosine (C18)

α-GalCer

B

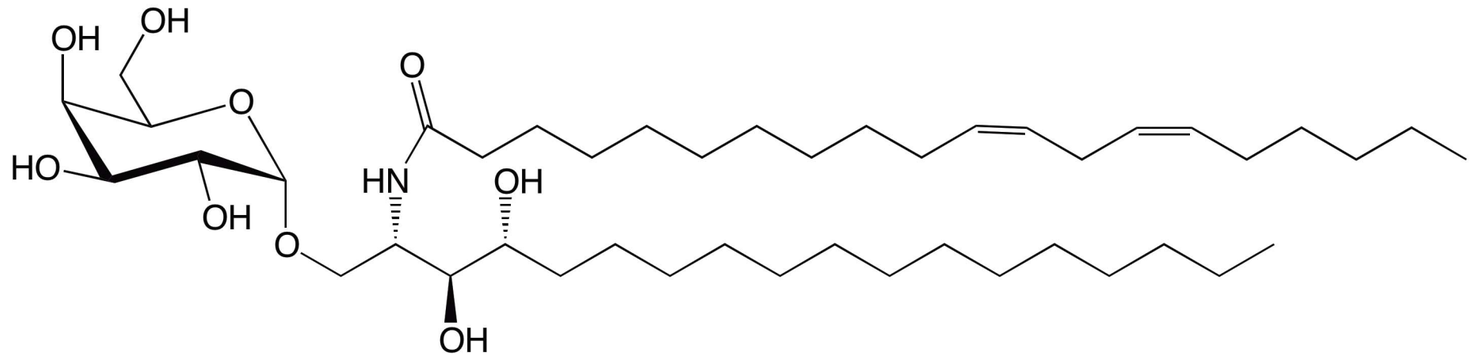

Acyl (C20:2)

Sphingosine (C18)

α-GalCer (C20:2)

C

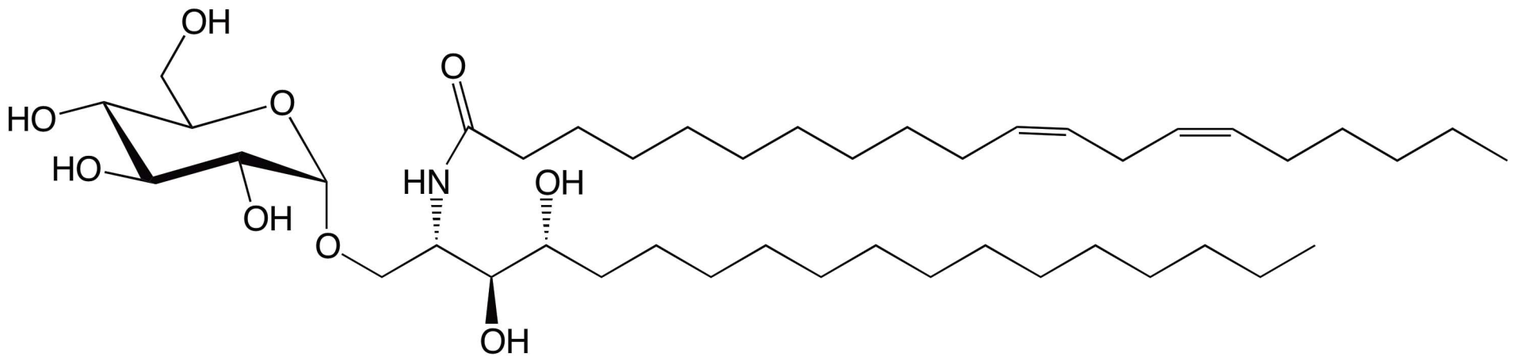

Acyl (C20:2)

Sphingosine (C18)

α-GlcCer (C20:2)

D

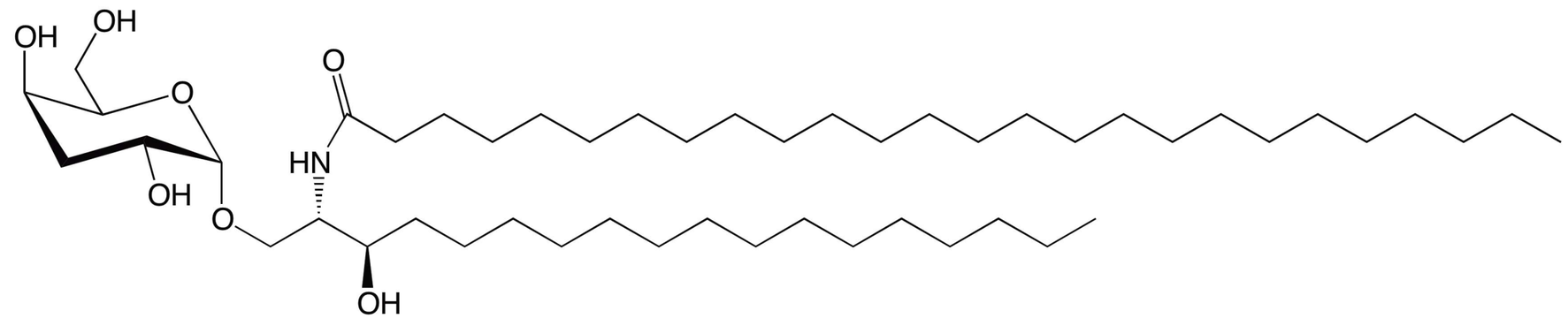

Acyl (C26)

Sphinganine
(C18:4´-deoxy)

3´,4´´-deoxy-α-GalCer

E

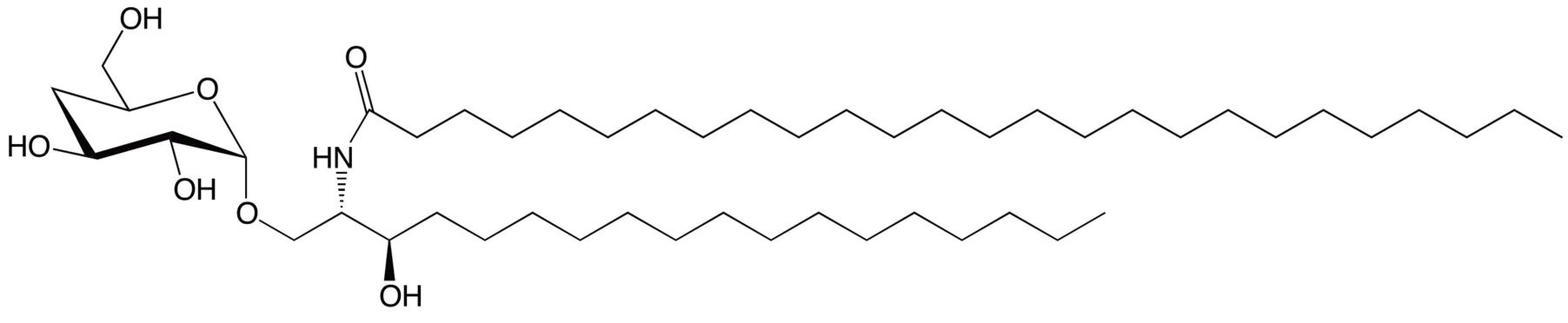

Acyl (C26)

Sphinganine
(C18:4´-deoxy)

4´,4´´-deoxy-α-GalCer

Figure 1

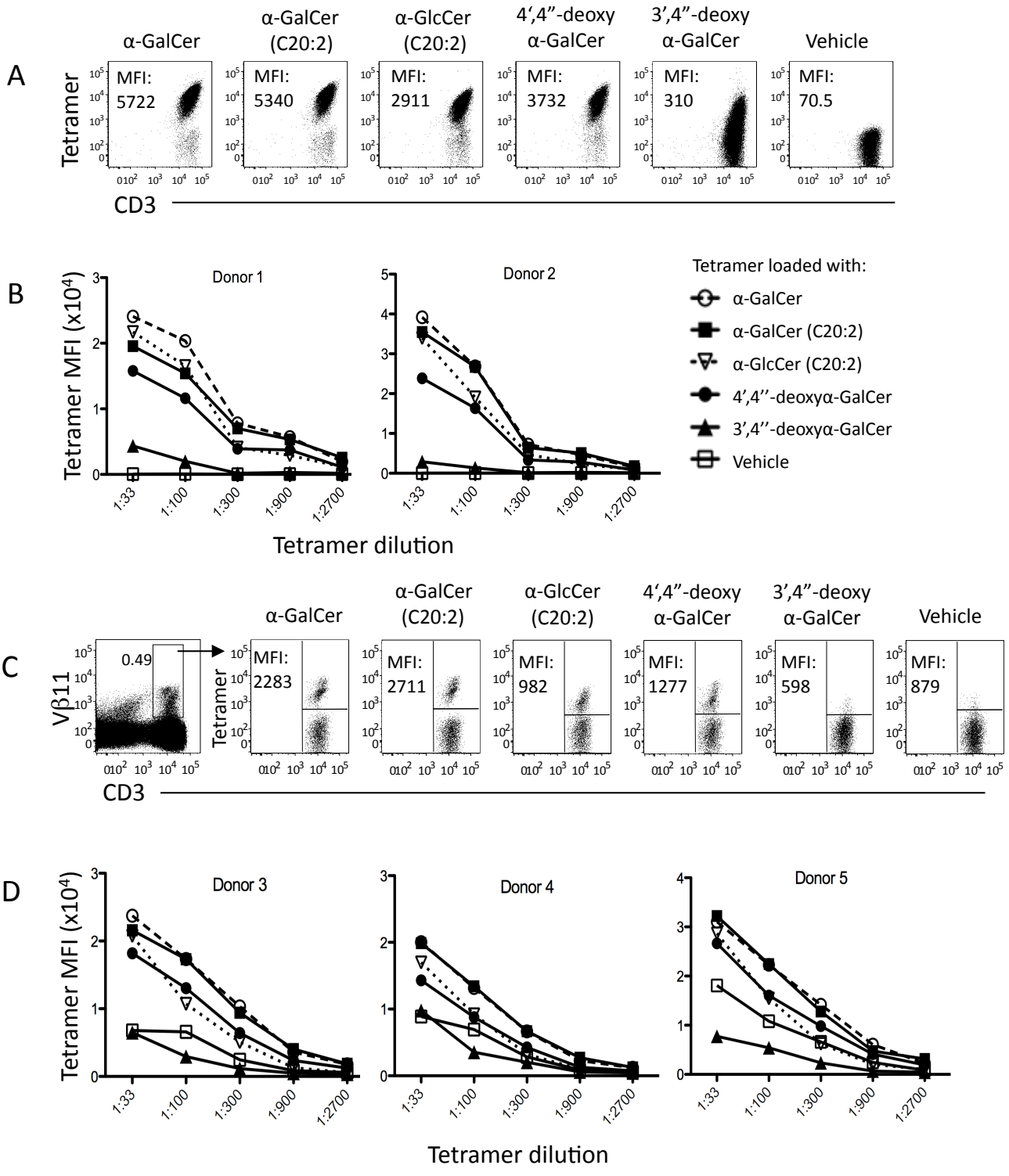
A
α-GalCer
α-GalCer (C20:2)
α-GlcCer (C20:2)
4',4''-deoxy α-GalCer
3',4''-deoxy α-GalCer
Vehicle
Tetramer
CD3
MFI: 5722
MFI: 5340
MFI: 2911
MFI: 3732
MFI: 310
MFI: 70.5
B
Donor 1
Donor 2
Tetramer MFI (x10⁴)
Tetramer dilution
1:33
1:100
1:300
1:900
1:2700
Tetramer loaded with:
α-GalCer
α-GalCer (C20:2)
α-GlcCer (C20:2)
4',4''-deoxyα-GalCer
3',4''-deoxyα-GalCer
Vehicle
C
Vβ11
0.49
Tetramer
CD3
α-GalCer
α-GalCer (C20:2)
α-GlcCer (C20:2)
4',4''-deoxy α-GalCer
3',4''-deoxy α-GalCer
Vehicle
MFI: 2283
MFI: 2711
MFI: 982
MFI: 1277
MFI: 598
MFI: 879
D
Donor 3
Donor 4
Donor 5
Tetramer MFI (x10⁴)
Tetramer dilution
1:33
1:100
1:300
1:900
1:2700

Figure 2

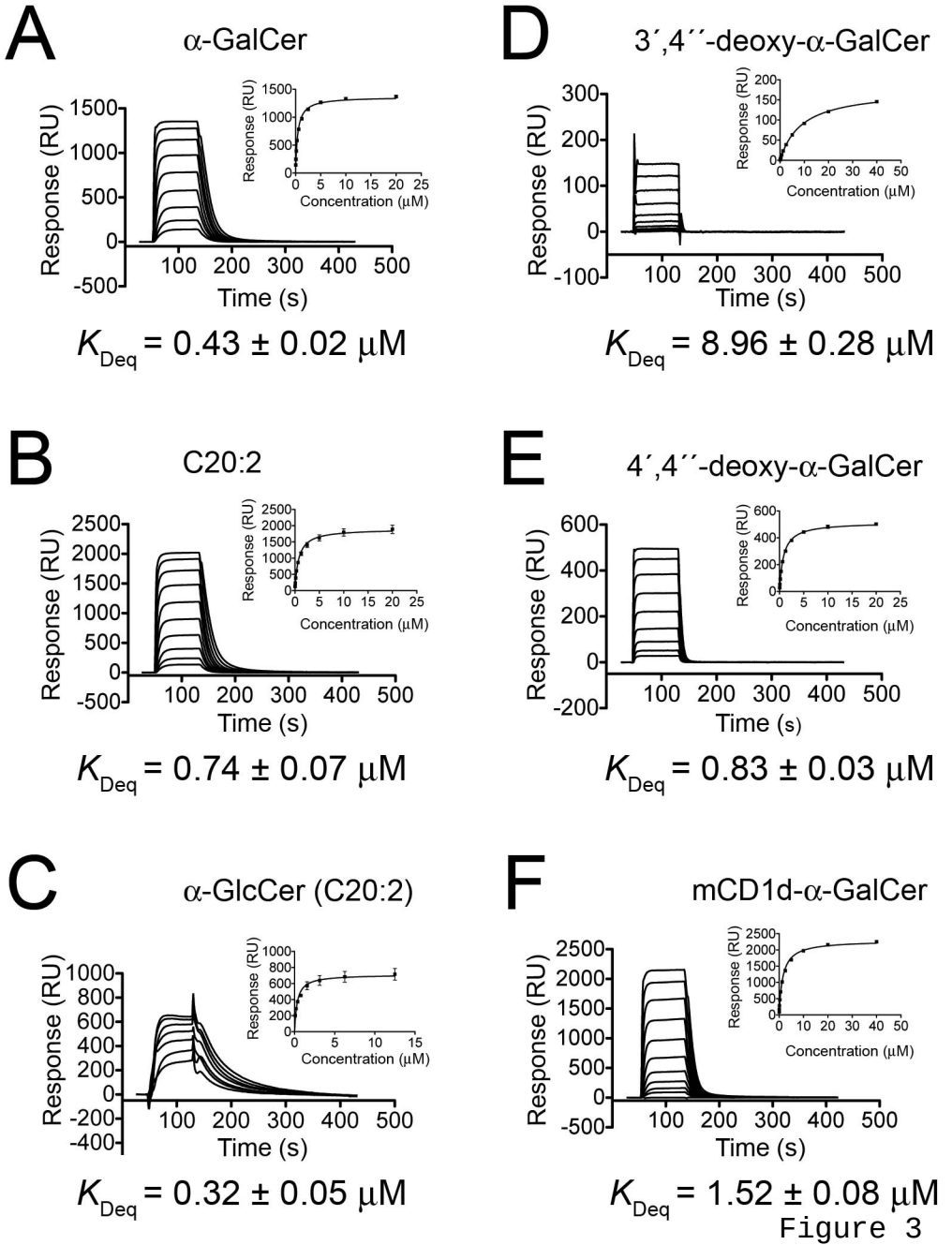
A
α-GalCer
Response (RU)
Time (s)
Concentration (μM)
K_{Deq} = 0.43 ± 0.02 μM
B
C20:2
K_{Deq} = 0.74 ± 0.07 μM
C
α-GlcCer (C20:2)
K_{Deq} = 0.32 ± 0.05 μM
D
3′,4′′-deoxy-α-GalCer
K_{Deq} = 8.96 ± 0.28 μM
E
4′,4′′-deoxy-α-GalCer
K_{Deq} = 0.83 ± 0.03 μM
F
mCD1d-α-GalCer
K_{Deq} = 1.52 ± 0.08 μM

Figure 3

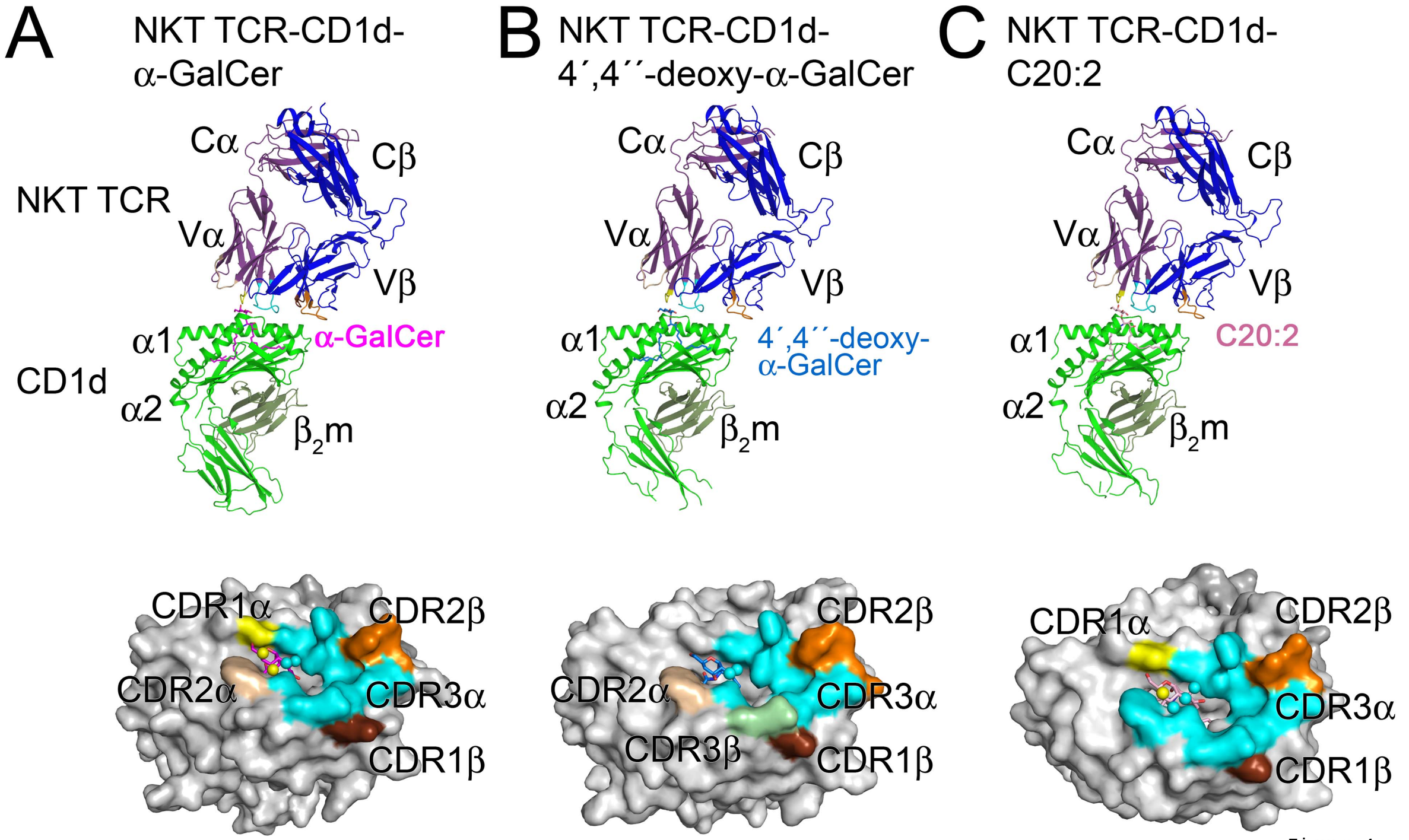
A
NKT TCR-CD1d-
α-GalCer
Cα
Cβ
NKT TCR
Vα
Vβ
α1
α-GalCer
CD1d
α2
β2m
B
NKT TCR-CD1d-
4´,4´´-deoxy-α-GalCer
Cα
Cβ
Vα
Vβ
α1
4´,4´´-deoxy-
α-GalCer
α2
β2m
C
NKT TCR-CD1d-
C20:2
Cα
Cβ
Vα
Vβ
α1
C20:2
α2
β2m
CDR1α
CDR2β
CDR2α
CDR3α
CDR1β
CDR2β
CDR2α
CDR3α
CDR3β
CDR1β
CDR1α
CDR2β
CDR3α
CDR1β

Figure 4

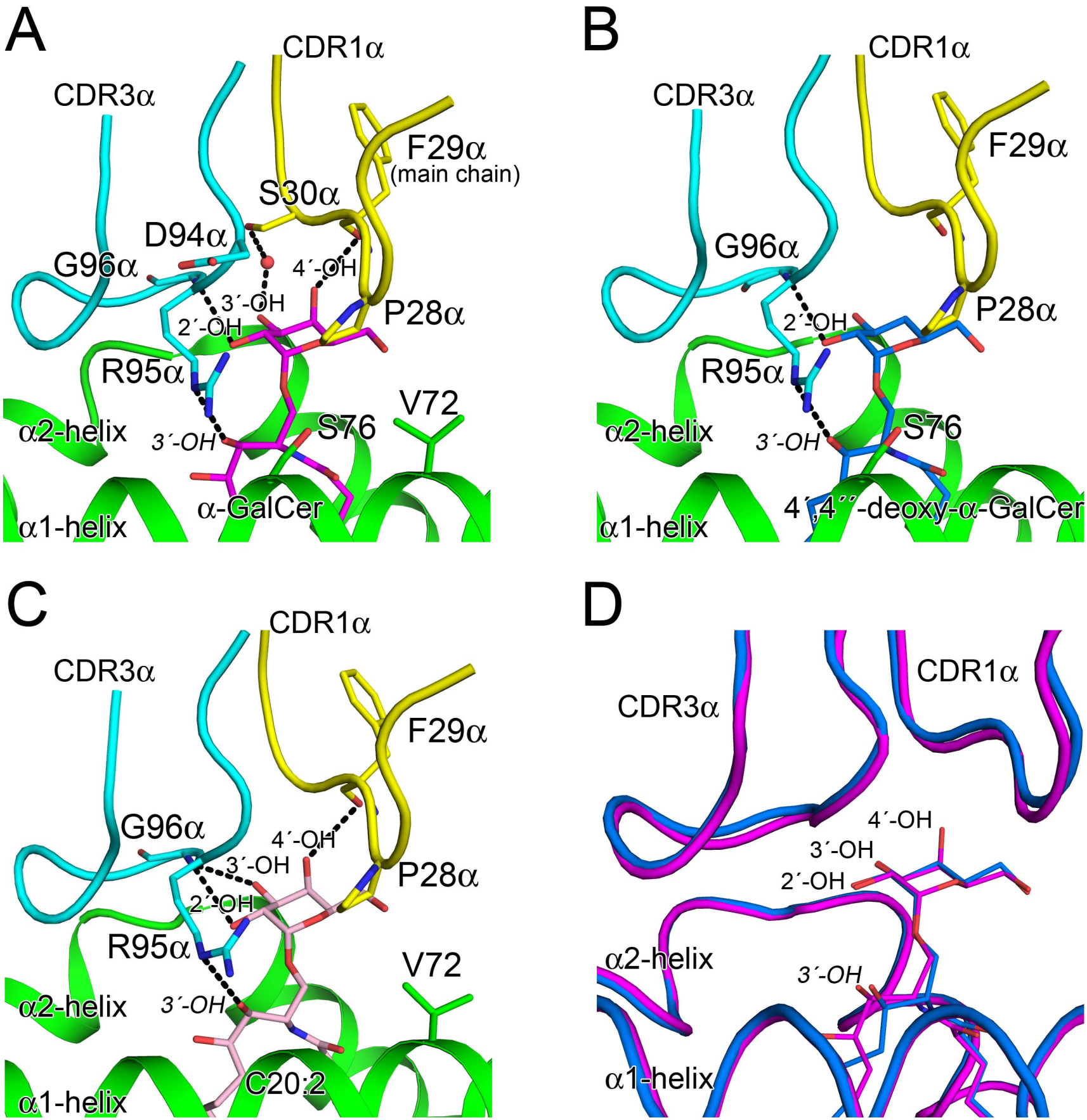
A
CDR1α
CDR3α
F29α
(main chain)
S30α
D94α
G96α
4´-OH
3´-OH
2´-OH
P28α
R95α
V72
α2-helix
3´-OH
S76
α-GalCer
α1-helix
B
CDR1α
CDR3α
F29α
G96α
P28α
2´-OH
R95α
α2-helix
3´-OH
S76
4´,4´´-deoxy-α-GalCer
α1-helix
C
CDR1α
CDR3α
F29α
G96α
4´-OH
3´-OH
P28α
2´-OH
R95α
V72
α2-helix
3´-OH
C20:2
α1-helix
D
CDR1α
CDR3α
4´-OH
3´-OH
2´-OH
α2-helix
3´-OH
α1-helix

Figure 5

University Library

MINERVA ACCESS

A gateway to Melbourne's research publications

Minerva Access is the Institutional Repository of The University of Melbourne

Author/s:
Wun, KS; Ross, F; Patel, O; Besra, GS; Porcelli, SA; Richardson, SK; Keshipeddy, S; Howell, AR; Godfrey, DI; Rossjohn, J

Title:
Human and Mouse Type I Natural Killer T Cell Antigen Receptors Exhibit Different Fine Specificities for CD1d-Antigen Complex

Date:
2012-11-09

Citation:
Wun, K. S., Ross, F., Patel, O., Besra, G. S., Porcelli, S. A., Richardson, S. K., Keshipeddy, S., Howell, A. R., Godfrey, D. I. & Rossjohn, J. (2012). Human and Mouse Type I Natural Killer T Cell Antigen Receptors Exhibit Different Fine Specificities for CD1d-Antigen Complex. JOURNAL OF BIOLOGICAL CHEMISTRY, 287 (46), pp.39139-39148. https://doi.org/10.1074/jbc.M112.412320.

Persistent Link:
http://hdl.handle.net/11343/44145